VANET Routing on City Roads Using Real-Time Vehicular Traffic Information

Josiane Nzouonta, Neeraj Rajgure, Guiling (Grace) Wang, *Member, IEEE*, and Cristian Borcea, *Member, IEEE*

***Abstract*—This paper presents a class of routing protocols called road-based using vehicular traffic (RBVT) routing, which outperforms existing routing protocols in city-based vehicular ad hoc networks (VANETs). RBVT protocols leverage real-time vehicular traffic information to create road-based paths consisting of successions of road intersections that have, with high probability, network connectivity among them. Geographical forwarding is used to transfer packets between intersections on the path, reducing the path's sensitivity to individual node movements. For dense networks with high contention, we optimize the forwarding using a distributed receiver-based election of next hops based on a multicriterion prioritization function that takes nonuniform radio propagation into account. We designed and implemented a reactive protocol RBVT-R and a proactive protocol RBVT-P and compared them with protocols representative of mobile ad hoc networks and VANETs. Simulation results in urban settings show that RBVT-R performs best in terms of average delivery rate, with up to a 40% increase compared with some existing protocols. In terms of average delay, RBVT-P performs best, with as much as an 85% decrease compared with the other protocols.**

***Index Terms*—Receiver-based next-hop election, road-based routing, vehicular traffic-aware routing.**

I. Introduction

VEHICULAR ad hoc networks (VANETs) are expected to support a large spectrum of mobile distributed applications that range from traffic alert dissemination and dynamic route planning to context-aware advertisement and file sharing [1]–[5]. Considering the large number of nodes that participate in these networks and their high mobility, debates still exist about the feasibility of applications that use end-to-end multihop communication. The main concern is whether the performance of VANET routing protocols can satisfy the throughput and delay requirements of such applications. This paper focuses on VANET routing in city-based scenarios.

Analyses of traditional routing protocols for mobile ad hoc networks (MANETs) demonstrated that their performance is poor in VANETs [6], [7]. The main problem with these protocols, e.g., ad hoc on-demand distance vector (AODV) [8] and dynamic source routing (DSR) [9], in VANET environments is their route instability. The traditional node-centric view of the routes (i.e., an established route is a fixed succession of nodes between the source and the destination) leads to frequent broken routes in the presence of VANETs' high mobility, as illustrated in Fig. 1(a). Consequently, many packets are dropped, and the overhead due to route repairs or failure notifications significantly increases, leading to low delivery ratios and high transmission delays.

One alternative approach is offered by geographical routing protocols, e.g., greedy–face–greedy (GFG) [10], greedy other adaptive face routing (GOAFR) [11], greedy perimeter stateless routing (GPSR) [12], which decouple forwarding from the nodes identity. These protocols do not establish routes but use the position of the destination and the position of the neighbor nodes to forward data. Unlike node-centric routing, geographical routing has the advantage that any node that ensures progress toward the destination can be used for forwarding. For instance, in Fig. 1(a), geographical forwarding could use node N2 instead of N1 to forward data to D. Despite better path stability, geographical forwarding does not also perform well in city-based VANETs [6], [13]. Its problem is that, oftentimes, it cannot find a next hop (i.e., a node that is closer to the destination than the current node). For example, as shown in Fig. 1(b), it can take road paths that do not lead to the destination. The recovery strategies in the literature are often based on planar graph traversals, which were shown to be ineffective in VANETs due to radio obstacles, high node mobility, and the fact that vehicle positions are constrained on roads rather than being uniformly distributed across a region [6].

A number of road-based routing protocols [6], [7], [13], [14] have been designed to address this issue. However, several protocols [6], [14] fail to factor in the vehicular traffic flow by using the shortest road path between the source and the destination. As depicted in Fig. 2, it is possible that the road segments on the shortest path are empty (or have network partitions). Other projects [13], [15]–[17] try to alleviate this issue by using historical data about average daily/hourly vehicular traffic flows. Unfortunately, historical data are not accurate indicators of the current road traffic conditions, because events such as road constructions or accidents that lead to traffic redirection are not rare.

This paper presents a class of road-based VANET routing protocols that leverage real-time vehicular traffic information to create paths consisting of successions of road intersections that have, with high probability, network connectivity among them. Furthermore, geographical forwarding allows the use

Manuscript received December 14, 2007; revised July 24, 2008 and December 23, 2008. First published February 3, 2009; current version published August 14, 2009. This work was supported in part by the U.S. National Science Foundation under Grant CNS-0520033, Grant CNS-0834585, and Grant CNS-0831753. Any opinions, findings, and conclusions or recommendations expressed in this material are those of the authors and do not necessarily reflect the views of the National Science Foundation. The review of this paper was coordinated by Dr. L. Cai.

The authors are with the Department of Computer Science, New Jersey Institute of Technology, Newark, NJ 07102 USA (e-mail: jn62@njit.edu; nmr2@njit.edu; gwang@cs.njit.edu; borcea@cs.njit.edu).

Color versions of one or more of the figures in this paper are available online at http://ieeexplore.ieee.org.

Digital Object Identifier 10.1109/TVT.2009.2014455

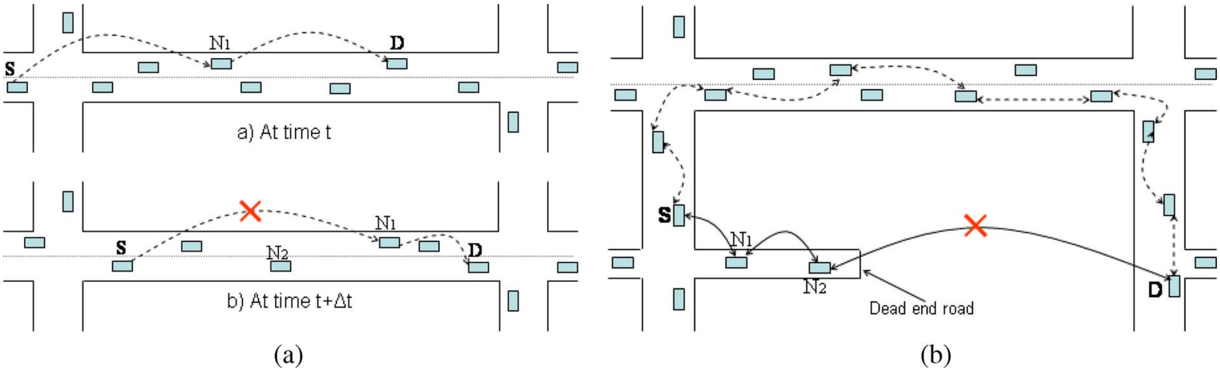

Fig. 1. Problems with traditional routing approaches in VANETs. (a) Routes that were established as fixed successions of nodes frequently break in highly mobile VANETs. Route (S, N1, D) that was established at time t breaks at time $t + \Delta t$ when N1 moves out of the transmission range of S. (b) Geographical routing can route packets toward dead ends, causing unnecessary traffic overhead in the network and longer delays for packets. Instead of forwarding data on the dotted path, geographical routing sends data to N1 and N2, following the shortest geographical path from S to D on a dead-end road.

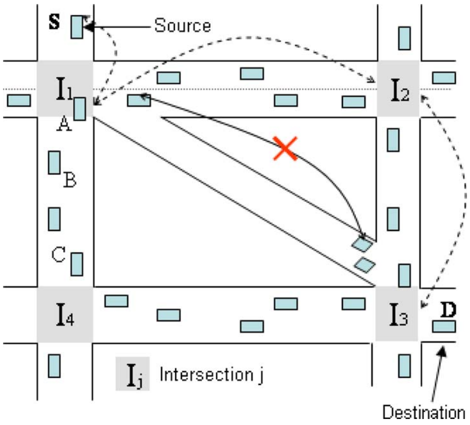

Fig. 2. Our solution creates a route (S, I1, I2, I3, D) using the road intersections. Since it considers the real-time vehicular traffic, our solution can avoid the shorter path (S, I1, I3, D) that would lead to a broken route. Once the road-based route is established, geographical forwarding is used to route data between any two intersections.

of any node on a road segment to transfer packets between two consecutive intersections on the path, reducing the path's sensitivity to individual node movements. Fig. 2 shows one example that illustrates the main idea of this class of routing, which we call road-based using vehicular traffic (RBVT) routing. The RBVT class of routing presents two main advantages: 1) adaptability to network conditions by incorporating real-time vehicular traffic information and 2) route stability through road-based routes and geographical forwarding. We present two RBVT protocols: 1) a reactive protocol RBVT-R and 2) a proactive protocol RBVT-P. RBVT-R discovers routes on demand and reports them back to the source, which includes them in the packet headers (i.e., source routing). RBVT-P generates periodical connectivity packets (CPs) that visit connected road segments and store the graph that they form. This graph is then disseminated to all nodes in the network and is used to compute the shortest paths to destinations.

Our initial NS-2 simulations with an IEEE 802.11 VANET showed that, when the wireless medium becomes congested, the overhead introduced by the periodic "hello" packets for maintaining the list of neighbors in geographical forwarding significantly degraded the end-to-end data transfer performance. To reduce this overhead, we propose a beaconless distributed receiver-based election of next hop, considering nonuniform radio propagation. This method uses a light modification of the request-to-send/clear-to-send (RTS/CTS) mechanism in the IEEE 802.11 standard. A multicriterion prioritization function is introduced to select the best next hop by using the distance between the next hop and the destination, the received power level (which could be affected by noise and channel fading), and the distance to the transmitter as parameters.

We evaluate the performance of the proposed protocols using two scenarios: 1) an urban environment with obstacles using periodic "hello" messages and the standard 802.11 medium access control (MAC) protocol (node movements are generated using the open-source microscopic traffic generator simulation of urban mobility (SUMO) [18], which has been validated against real vehicular traces) and 2) an urban environment without obstacles, using the proposed forwarding optimization for the RBVT protocols. This scenario tests the protocols in high-contention environments. In these tests, we used a vehicular traffic generator that we developed based on the car-following model proposed by Gipps [19], [20]. This model enables vehicles to move at the maximum safest speed while avoiding collisions.

The simulation results show that the RBVT protocols outperform existing protocols in both studied scenarios. In terms of successful data delivery, RBVT-R performed best, with an increase of as much as 40% compared with AODV and 30% compared with GSR using the IEEE 802.11 standard. In terms of the average delay, RBVT- P performed best, with delays of as much as 85% lower than existing solutions. The proposed forwarding optimization provided noticeable improvements in the high-contention scenario. The scenario with obstacles yielded better performance, even without using the optimization. This case was the result of lower contention in the network and the fact that RBVT protocols forward data along the roads and not across the roads.

The rest of this paper is organized as follows. Section II presents the two RBVT protocols. Section III describes the optimized forwarding mechanism. Section IV presents the simulation results. The related work is reviewed in Section V, and this paper is concluded in Section VI.

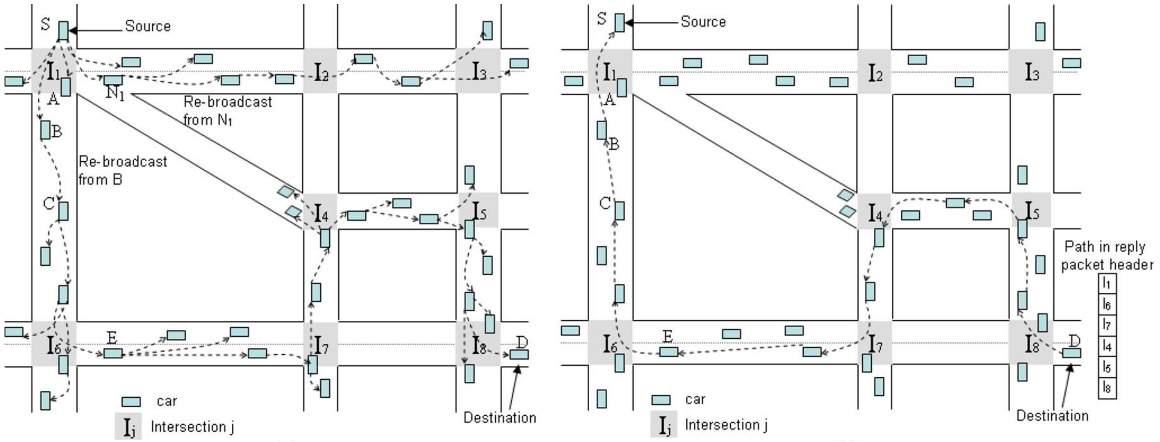

(a) (b)

Fig. 3. Route establishment in RBVT-R. (a) A source node uses our improved flooding mechanism to send a route discovery packet in the network to find the destination. The route discovery packet is broadcast along the roads and stores the traversed intersections in its header. (b) The destination unicasts a route reply packet back to the source. The reply follows the route that was stored in the route discovery packet, and geographical forwarding is used between intersections.

II. RBVT Protocols

The RBVT routing protocols leverage real-time vehicular traffic information to create road-based paths. RBVT paths can be created on demand or proactively. We designed and implemented two RBVT protocols, each illustrating a method of path creation: 1) a reactive protocol RBVT-R and 2) a proactive protocol RBVT-P. The RBVT protocols assume that each vehicle is equipped with a GPS receiver, digital maps (e.g., Tiger Line database [21]), and a navigation system that maps GPS positions on roads. Vehicles exchange packets using short-range wireless interfaces such as IEEE 802.11 [22] and dedicated short-range communication (DSRC) [23].

A. RBVT-R: Reactive Routing Protocol

RBVT-R is a reactive source routing protocol for VANETs that creates road-based paths (routes) on demand by using "connected" road segments. A connected road segment is a segment between two adjacent intersections with enough vehicular traffic to ensure network connectivity. These routes, which are represented as sequences of intersections, are stored in the data packet headers and are used by intermediate nodes to geographically forward packets between intersections.

1) Route Discovery (RD): When a source node needs to send information to a destination node, RBVT-R initiates a route discovery process, as illustrated in Fig. 3(a). The source creates an RD packet, whose header includes the address and location of the source, the address of the destination, and a sequence number. We assume unique addresses for nodes. RD is flooded in the region around the source to discover a route toward the destination. The flooding is necessary, because RBVT-R does not assume a location service that can be queried to find out the location of the destination. For scalability reasons, the flooding region is limited by a time-to-live (TTL) value that is set in the header.

To reduce the effects of the broadcast storm problem [24], RBVT-R uses an improved flooding mechanism similar to [25]. If a node receives an RD packet with the same source address and sequence number with a previously received packet, it discards the RD packet. When a node receives a new RD, it does not directly rebroadcast this packet; the node holds the packet for a period of time inversely proportional to the distance between itself and the sending node. Once the waiting period is over, a node rebroadcasts the RD packet only if it did not notice that this packet was rebroadcast by nodes that are located farther on the same road segment. This way, farther nodes can first rebroadcast the request, thus ensuring faster progress and less traffic in the network.

In RBVT-R, the route is gradually built. Initially, the route stored in the RD packet is an empty list. When a node receives the RD packet for the first time, it checks if it is located on a different road segment from the transmitter of the packet. If so, the receiving node appends to the route list the road intersections that were "traversed" by the RD packet from the transmitter position. We illustrate the route creation process using Fig. 3(a). The source vehicle S creates an RD packet to discover a route to destination D. S adds its own position in the packet and broadcasts it. Both nodes A and B receive the packet on segment I_1–I_6, but only B will rebroadcast it in the improved flooding mechanism. Before this rebroadcast, B appends intersection I_1 to the route in the header of the packet. However, when C receives the RD packet, it will not update the route, because C is on the same road segment with B. A new intersection I_6 is added at node E. This process continues until the packet reaches the destination or the TTL expires.

The RD packet may sometimes be received by nodes on parallel streets. In this case, the RD packet is updated only if the sequence of intersections that were implicitly traversed can be determined. If this condition is not possible, we prevent, in our implementation, those nodes from updating the RD packets. The route structure is stored in the header of the RD packet; thus, the number of intersections that can be appended to a route is limited by the size of the IP packet header options and the number of bytes for identifying each road intersection. Techniques such as hierarchical naming of intersections (i.e., identifying the city and then the intersections within the city) can increase the maximum number of intersections that are stored in RD.

2) Route Reply (RR): Upon receiving the RD packet, the destination node creates an RR packet for the source. The route that is recorded in the RD header is copied in the RR header. As shown in Fig. 3(b), this route defines a connected path, which is composed of road intersections, from the source to the destination. The destination also adds its current position in the RR header. The RR packet is forwarded along the road segments that are defined by the intersections in its header. Geographical forwarding is used between intersections to take advantage of every available node on the path. The destination may receive duplicates of an RD packet. A new reply is generated only if the newly received packet contains a route of better quality. The quality of a route can be expressed using a combination of metrics such as node density on the road segments, the number of lanes, and traffic-flow rates. In the current implementation, the fewer the number of intersections, the better the route. Upon receiving the RR packet, the source starts sending data. Each data packet stores the route in its header, and it is geographically forwarded along this route. Protocol 1 presents the pseudocode for the RD and RR phases.

Protocol 1: RD and RR in RBVT-R at node n_i

Notation:

n_S and n_D: ID of the source and the destination

$Path$ and $TempPath$: Best and temporary paths from n_S to n_D

$|Path|$: Path length

$RS(n_i)$: Road segment where node n_i is located

α: Waiting-time parameter

RD: RD packet

RR: RR packet

```
Upon receiving RD($n_S, n_D, TempPath$) from $n_j$
if ($n_i == n_D$)&($|TempPath| \leq |Path|$) then
    $Path = TempPath$
    Send RR($n_D, n_S, Path$)
    Return
end if
if RD not seen before then
    if ($RS(n_i) \neq RS(n_j)$)&($RS(n_i) \notin TempPath$) then
        Add $RS(n_i)$ to $TempPath$
    end if
    Set timer $= \alpha * distance(n_j, n_i)$
else
    if $RS(n_i) == RS(n_j)$ then
        Cancel timer /*$n_j$ is a better broadcast node */
    end if
end if

Upon timeout
Broadcast RD($n_S, n_D, TempPath$)

Upon receiving RR($n_D, n_S, Path$) from $n_j$:
if $n_i == n_S$ then
    Store $Path$
    Forward $Data(Path)$
else
    Forward RR($n_D, n_S, Path$)
end if
```

3) Route Maintenance: Existing routes are updated to adapt to the movements of the source and the destination over time and to repair broken paths. Sources and destinations are moving vehicles; thus, the route that was created during the RD phase is not expected to remain constant. We use a dynamic route updating technique at the source to keep the route consistent with the current road segment positions of the source and the destination nodes. For instance, if node S in Fig. 3(b) moves to segment I_1–I_6, I_1 is no longer a valid intersection along the route and should be removed. This change takes place at the source, which also informs the destination of the new path using route update (RU) control packets. Similarly, node D may move to road segment I_5–I_8. When this happens, I_8 should be removed from the list of intersections in the route. Consequently, the destination sends an RU packet to the source. If this update is received at the source, it means that the route is valid, and it can, therefore, be used for future data transmissions.

In some situations, the vehicle node may transmit the RU packet before changing the road segment. For example, if a vehicle node is about to make a turn that will result in the addition of an intersection to the path, the presence of obstacles may temporarily cause a loss in connectivity [26], which may prevent the successful transmission of the update packet. To avert this problem, vehicle nodes with RBVT-R can transmit the RU packet before the turn to the new segment is complete.

A route error occurs when no forwarding node can be found to reach the next intersection in the route. In this case, the node that detected the problem unicasts a route error packet to the source. We observed that, sometimes, broken routes are only temporary. Therefore, to reduce the flooding associated with the RD process, the source does not generate a new RD packet as soon as it receives a route error notification. Upon such a notification, it puts the respective route on hold for a certain timeout. Packets toward that destination are queued until the expiration of the hold timeout. The source then attempts to use the same route. An RD is generated only after a few consecutive route errors.

B. RBVT-P: Proactive Road-Based Routing

RBVT-P is a proactive routing algorithm that periodically discovers and disseminates the road-based network topology to maintain a relatively consistent view of the network connectivity at each node. Each node uses this (near) real-time graph of the connected road segments to compute shortest paths to each intersection. RBVT-P assumes that a source can query a location service (e.g., GLS [27]) to determine the position of the destination when it needs to send data.

1) Topology Discovery: Proactive routing algorithms [28] use various forms of flooding to discover and update the network topology. To keep up with VANET's mobility, flooding may be required quite often, and the routing overhead would lead to heavy congestion in the network. In RBVT-P, however, we can limit flooding frequency, because we are mainly

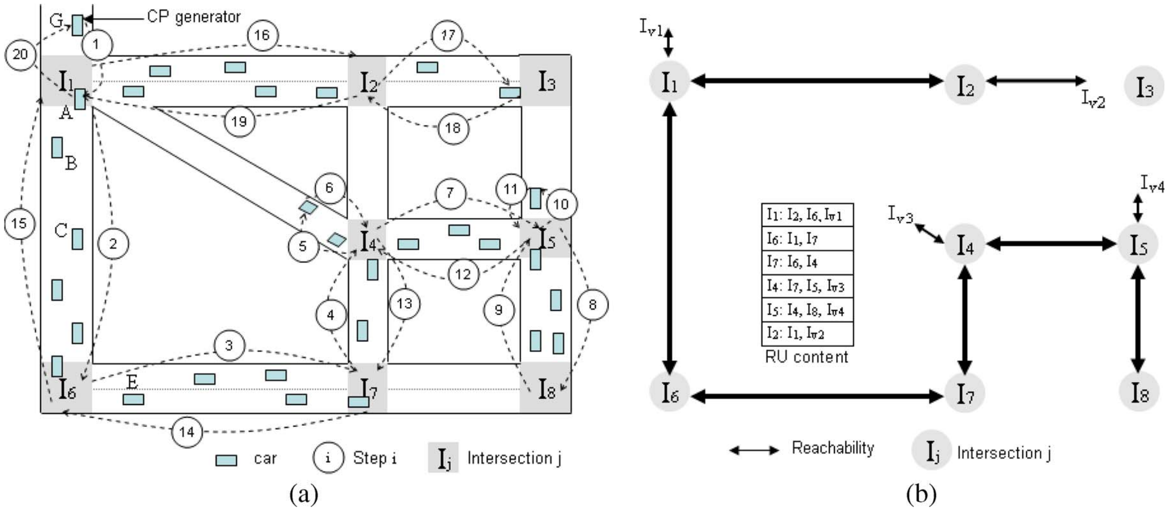

Fig. 4. Route establishment in RBVT-P. (a) Generator nodes periodically unicast CPs to discover the road-based network topology. The path of one CP is depicted step by step as it visits and records all road segments with enough vehicular traffic to maintain connectivity between endpoints. As shown between intersection I_4 and I_1, the CP creates a virtual intersection when a road segment has partial traffic, but a network partition precludes it from reaching the next intersection. (b) The CP returns to the segment of its generator with the network topology graph shown in this figure, which contains all the road segments with traffic on them. Note that segments with partial traffic are considered by adding virtual intersections. Then, a route-update packet that contains this graph is disseminated to all nodes in the network. Upon receiving a route update, each node updates its routing table and recomputes the shortest paths to all intersections.

interested in discovering the road-based network topology. More precisely, the goal of RBVT-P is to capture the real-time view of the traffic on the roads. Thus, the fact that the connectivity between certain nodes on a road segment changes over time does not matter as much, as long as that road segment remains connected. This situation is highly probable on roads with relatively dense vehicular traffic.

The road-based network topology is constructed using connectivity packets (CPs) that were unicast in the network. CPs traverse road segments and store their endpoints (i.e., intersections) in the packet. CPs are periodically generated by a number of randomly selected nodes in the network. Each node independently decides whether it will generate a new CP based on the estimated current number of vehicles in the networks, the historic hourly traffic information, and the time interval since it has last received a CP update. When creating a new CP, a node defines the road-based perimeter of the region to be covered by the CP and stores it in the CP. This step is necessary both to limit the time spent by the CP in the network, which implicitly defines the freshness of its information, and to ensure that this information fits in one packet. CPs traverse the road map using an algorithm that was derived from a depth-first search (DFS) graph traversal but, unlike DFS, the road intersections (vertices) are not added to the stack at the beginning of the traversal. Rather, vertices are progressively added to the CP stack as the CP reaches adjacent road segments. We use flags (i.e., U for unreachable, R for reachable, and I for initialized) to keep track of the state of the intersections in the CP stack. Network partitions may preclude the CP from visiting the entire graph. We discuss this issue in Section II-B4. Fig. 4(a) illustrates how one CP sequentially visits connected road segments and returns with the topology information to its generator segment. The CP traversal ends at the road segment of the initiator. Any vehicle that first receives the CP on that segment after all marked intersections have been visited will disseminate the CP content.

2) Topology Dissemination: The network topology information in the CP is extracted and stored in an RU packet that is disseminated to all nodes in the network (i.e., in the region covered by the CP). Fig. 4(b) shows the CP/RU content associated with the topology in Fig. 4(a). The RU is marked with a timestamp to indicate the freshness of its information (i.e., because nodes have GPS receivers, they can use the GPS time, which varies insignificantly among different receivers). Upon receiving an RU packet, nodes update their local routing table to reflect the newly received information.

Each node maintains a routing table with entries of the form

$$\langle Intersection_i, Intersection_j, State, \\ Timestamp, Entry\_timeout\rangle$$

where $state$ is equal to R or U. R means that the intersection is reachable, whereas U means that it is unreachable. The $timestamp$ is taken from the RU packet during the update. The $entry\_timeout$ is a function of the CP generation period and allows the node to purge old information when no new updates about certain intersections are received. When a node receives an RU, it does not replace its entire routing table with the new topology, but rather, it updates its routing table on a segment-by-segment basis. This type of update allows each node to aggregate information from multiple RUs into its local routing table. Note that it is possible to receive information from multiple RUs that visited overlapping regions. Protocol 2 presents the pseudocode for topology discovery and dissemination.

```
Protocol 2: Topology discovery and dissemination in RBVT-P at node $n_i$
Notation:
    $n_O$: ID of the node that originated the CP
    $I_l$: Intersection $l$
    $I_{n_i}$: Intersection that is closest to $n_i$
    $\langle I_l, I_m \rangle$: Road segment between consecutive intersections $I_l$ and $I_m$
    $Stack$: Stack of road segments that will be visited
    $S$: Set of all road segments
    $RS(n_i)$: Road segment where node $n_i$ is located
    $\alpha$: Waiting-time parameter
    CP: CP
    RU: RU packet

Upon receiving CP($n_O$):
if proximity($n_i, I_l$) then
    for each $\langle I_l, I_k \rangle$ do
        if $\langle I_l, I_k \rangle \notin Stack$ then
            Add $\langle I_l, I_k \rangle$ to $Stack$
        end if
    end for
    if $I_{n_i} == I_{n_O} \& Stack == \phi$ then
        Broadcast RU($n_i$)
        Return
    end if
    if $RS(n_i) == \langle I_l, I_m \rangle$ & (all $\langle I_m, I_k \rangle$ in $Stack \|$ marked in $S$) then
        Mark the reachability of $\langle I_l, I_m \rangle$ in $S/*$ R—reachable; U—unreachable $*/$
        Remove $\langle I_l, I_m \rangle$ from $Stack$
    end if
    Read $\langle I_l, I_m \rangle$ from the top of $Stack$
    Forward CP($n_O$) toward $I_m/*$ Send to the next hop toward $I_m */$
end if

Upon receiving RU($n_O$) from $n_j$:
if RU($n_O$) not seen before then
    Update the local routing table with RU($n_O$) data
    Set timer $= \alpha * distance(n_j, n_i)$
else
    if $RS(n_i) == RS(n_j)$ then
        Cancel timer
    end if
end if

Upon timeout
Broadcast RU($n_O$)
```

3) Route Computation: A source node computes the shortest path to the destination by using only road segments that are marked as reachable in its routing table. The sequence of intersections that denote the path is added to the header of each data packet. This header includes the timestamp that is associated with the route to allow for freshness comparisons at intermediate nodes.

Once the route is computed, RBVT-P uses loose source routing to forward data packets to improve the forwarding performance. The idea is to quickly forward the packet when the intermediate nodes have the same or older information than the source and, at the same time, take advantage of fresher information when available.

4) Route Maintenance: Intermediate nodes with fresher information update the path in the header of data packets. In case of a route break, the intermediate node switches to geographical routing, which is used until the packet reaches a node that has fresher information, and consequently, a new route is stored in the packet header.

One important consideration is the number of CPs that are needed in the network. RBVT-P generates multiple CPs from different positions in each update period. This condition is needed to ensure redundancy in the event of CP losses or network partitions, which could frequently happen in highly volatile VANETs. Indeed, in case of a network partition, the nodes in the partition from which the CP was generated would still receive updated information on that part of the network, as well as knowledge of disconnections. However, nodes in any other partition would no longer receive updates until the partition is bridged. Thus, there is a need to instantiate CPs from different positions in the network. The presence of multiple CPs, however, raises consistency issues, because a node may receive RU updates from multiple sources. This problem is solved using the RU timestamps, as we have previously described.

III. Forwarding Optimization

Our initial simulation results with RBVT protocols showed that, as the network became congested, the overhead traffic from periodic "hello" messages negatively created an impact on the end-to-end data transfers. This section presents our solution to this problem, i.e., a distributed next-hop election method, which significantly increases the average data delivery ratio by reducing the overhead associated with the selection of the next-hop node in congested networks.

In RBVT, geographical forwarding is used to transfer data packets between intersections. In previous works on geographical or position-based forwarding [10]–[12], each forwarding node picks the next hop by using its list of neighbors and their geographical positions. The next hop is chosen in such a way that the forwarding progress is maximized (e.g., typically, this is the neighbor closest to the destination). This process continues until the packet reaches the destination. Therefore, to successfully choose next hops, it is vital for each en-route node to keep a precise neighbor list. If the lists are not accurate, the best next hop could be missed, or even worse, a node that is already out of the transmission range could be chosen. Maintaining up-to-date lists requires frequent "hello" packet broadcasting. However, this broadcasting results in a large communication overhead.

We propose a solution that was inspired by the receiver-based relay election approaches (e.g., [29]–[31]) in ad hoc and sensor networks to eliminate "hello" packets. In these approaches, the sender broadcasts a control packet that informs its neighbors about a pending data packet transmission. Each receiver uses certain criteria to determine if it should elect itself as a next-hop candidate, and if so, it computes a waiting time. This waiting time is used to allow better receivers to answer first. If a receiver does not overhear a better candidate before its waiting time expires, it informs the sender that it is the best next hop.

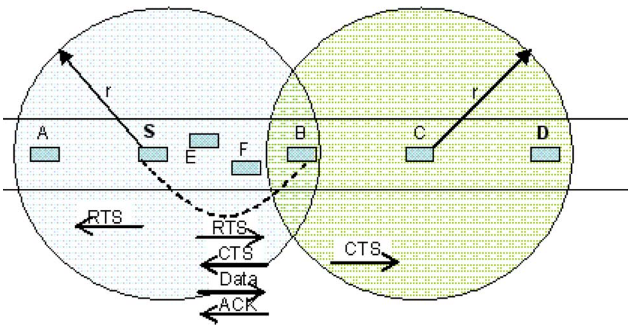

Fig. 5. RTS/CTS exchange in the IEEE 802.11 with DCF standard.

The current implementations of these approaches use one criterion for computing the waiting time, i.e., the distance between potential next hops and the destination. This method works well under the unit-disk assumption (i.e., the transmission range is a circle of a fixed radius). However, previous studies (e.g., [32]) have shown that real wireless radios do not follow the unit-disk assumption. This is particularly true in vehicular networks where buildings and other obstacles create an impact on radio propagation through signal fluctuations and fading. In this context, selecting the neighbor that optimizes the forward progress alone does not guarantee an optimal selection of the next hop [33].

The method proposed here accounts for nonuniform radio propagation that uses two additional criteria: 1) optimal transmission area and 2) received power. Furthermore, our next-hop election protocol piggybacks its data on the IEEE 802.11 RTS/CTS frames [22], thus introducing no overhead. To help with the understanding of this protocol, we continue the presentation with a brief overview of the IEEE RTS/CTS mechanism.

A. 802.11 RTS/CTS Background

In the IEEE 802.11 with distributed coordination function (DCF) standard, the RTS and CTS frames are used to address the hidden terminal problem that is inherent to wireless communications. This problem and the functionality of RTS/CTS frames are illustrated in Fig. 5. In this example, both node S and node C are node B's neighbors. When S sends a frame to B, C should not send any frame to B; otherwise, there would be a collision at B. However, node C is out of the communication range of node S, and it does not detect a busy channel while S is transmitting. Once node C starts its transmission, a collision happens at B, which cannot be detected by S until after it times out without receiving an acknowledgment from B.

IEEE 802.11 with DCF addresses the hidden terminal problem by deploying the RTS/CTS exchange. Before a node transmits a frame, it sends a very short RTS frame to the intended receiver, including the transmission time of the follow-up data and acknowledgment frames. The receiver broadcasts a CTS message, which is received by all its neighbors, once it receives the RTS with the needed channel clear time. The neighbors will consequently defer their transmissions until this transmission is completed. In the example, node C will never send to node B while node S is sending to node B, because node C has heard the CTS from node B. Node C will wait for the time specified in the CTS to guarantee that the transmission from S to B is successful.

B. Election Using RTS/CTS

RBVT leverages the RTS/CTS exchange to replace the sender selection of the next hop with a receiver self election and implicitly eliminates the overhead associated with frequent "hello" messages in geographical forwarding in congested networks. In essence, broadcasts of RTS frames become requests for next-hop self election. RTS frames are modified to carry the position of the sender and the position of the target destination, which are used during the self election. RTS frames also carry a flag to indicate to all receiving nodes that they should process and, possibly, answer the frame (in the original mechanism, only the intended receiver processes and answers an RTS frame).

In particular, each node that receives the modified RTS frame calculates a waiting time, after which it will send a CTS frame back to the sender. The waiting time is an indicator of how good the node is a forwarding candidate; i.e., the shorter the waiting time is, the better candidate the node becomes. Section III-C explains how this waiting time is calculated. A CTS from one of the receivers indicates that a better candidate exists, and no candidate receivers that overhear it will reply. The sender receives the CTS from the best next-hop candidate and forwards the data frame to this node, which then acknowledges the data frame. The detailed protocol is presented in Protocol 3.

```
**Protocol 3**: Self-election algorithm at node $n_i$
Notation:
    $t_{\mathrm{DATA}}$, $t_{\mathrm{CTS}}$, $t_{\mathrm{RTS}}$, and $t_{\mathrm{ACK}}$: time to transmit the data
    frame, CTS, RTS, and ACK
    $t_i$: waiting time of node $n_i$
    $loc_i$: location of node $n_i$
    $loc_D$: location of the destination
    $n_S$: ID of the sender that looks for the next hop

Upon receiving RTS$(loc_s, loc_D, t_{\mathrm{DATA}})$ from node $n_s$:
1: Call the waiting function and calculate $t_i$
2: Set the timer to $t_i$
3: Defer transmissions, if any, for $t_{\mathrm{DATA}} + t_{\mathrm{RTS}}$

Upon receiving an CTS$(n_j, n_s, t_{\mathrm{DATA}})$ from $n_j$ before the
timeout
4: Cancel the timer $/ * n_j$ is the best next-hop candidate $*/$
5: Defer transmissions, if any, for $t_{\mathrm{DATA}}$
Upon overhearing DATA from node $n_s$
6: Defer transmissions, if any, for $t_{\mathrm{ACK}}$

Upon timeout:
7: Broadcast CTS$(n_i, n_S, t_{\mathrm{DATA}}) / * n_i$ is the best candidate
$*/$
```

Fig. 6 shows an example that illustrates this protocol. Sender n_S needs to forward a data frame to the best next hop that is en route to destination D. It broadcasts an RTS frame by specifying its own location, the location of destination D, and

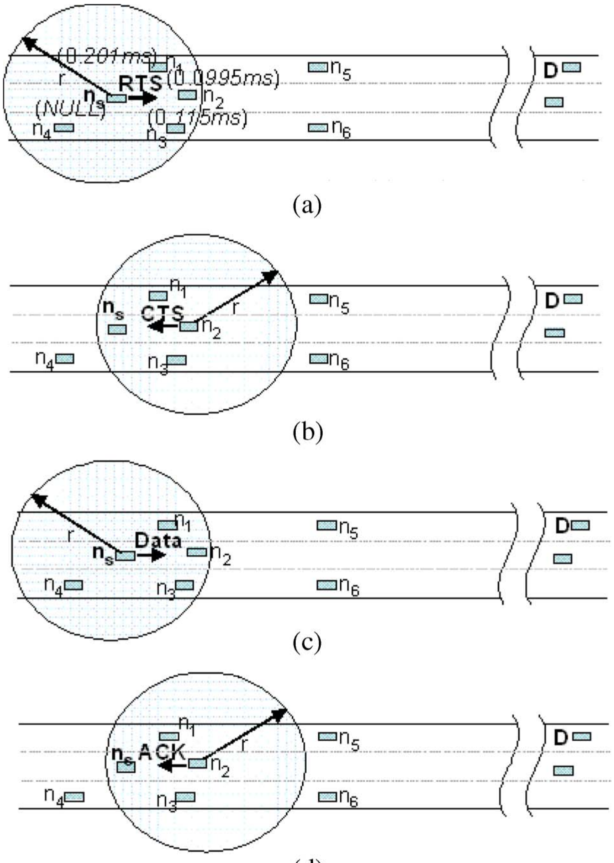

(a)

(b)

(c)

(d)

Fig. 6. Next-hop self-election example. (a) RTS broadcast and waiting-time computation. (b) CTS broadcast. (c) Data frame. (d) ACK unicast.

the transmission time of the data frame. Nodes n_1, n_2, and n_3 hear the RTS, calculate their waiting time, and set their timers to wait before replying to n_S with CTS. Note that n_4 does not perform the computation, because it is farther from the destination compared to the sender. Node n_2 has the shortest waiting time and replies with the CTS first. Once n_1 and n_3 overhear the CTS from n_2, they will cancel their timers. In addition, all the neighbors of n_2, will know that they should not send any frame to n_2 until it completes the transmission. Once n_S receives the CTS from n_2 it will send the data frame to n_2. At the same time, all of n_S's neighbors that overhear the data frame learn that they should not send any frame to n_S until n_2 finishes sending the acknowledgment to n_S. This example shows how this forwarding method can effectively choose the next hop without any "hello" message overhead.

C. Waiting Function

Determining the best next hop depends on the waiting time. An effective calculation of this waiting time should meet three objectives: 1) The waiting time of the best next-hop candidate is the shortest time such that this node replies first; 2) the waiting time difference between the best next-hop candidate and the second best candidate is large enough such that collisions are minimized between nearby nodes; and 3) the waiting time is as short as possible to avoid unnecessary delays. To achieve these goals, we first identify three key parameters—forward progress, optimal transmission area, and received power—that characterize the best next hop and then incorporate them with different weights into a low-complexity function that computes the waiting time.

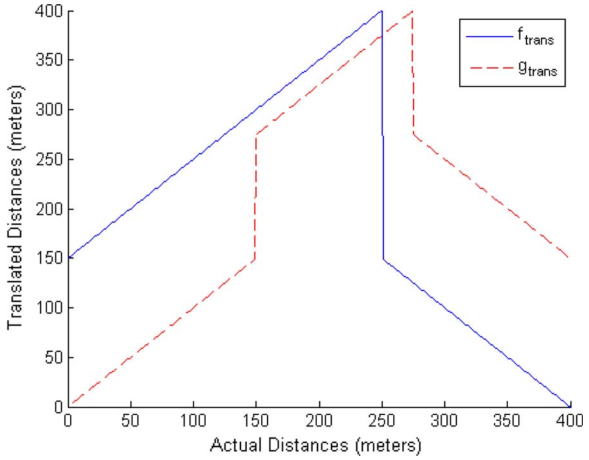

Fig. 7. Sample translation functions for the optimal transmission area.

1) Function parameters: The *forward progress* d_i of a node N_i from a sender S is defined as $d_i = d_{SD} - d_{N_iD}$, where d_{SD} is the distance between the sender S and the destination D, and d_{N_iD} is the distance between N_i and D. This parameter is commonly used in the geographical forwarding of single-criterion receiver-oriented schemes [29], [30], [34]. It denotes the actual progression that the packet made toward the destination if N_i would be the next hop. A node with d_i that is closest to d_{SD} is the node closest to the destination.

The *optimal transmission area* f_i of a node N_i describes the probability that the node can successfully receive the sender's data packet. Wireless channels are error prone; thus, a node that is located much farther than the nominal transmission range may not successfully receive long data frames, although it can receive short RTS frames without errors. This situation could happen because real wireless radios do not follow the unit-disk assumption [32].

We deploy a translation function to express the optimal transmission area. The function takes the distance to the sender as input and outputs the distance to the optimal transmission area. Sample graphs for two translation functions are depicted in Fig. 7, and one of these functions is defined as follows:

$$f_{trans}(x) = \begin{cases} x + d_{trans}, & \text{if } x \le d_{opt} \\ -x + d_{\max}, & \text{if } x > d_{opt} \end{cases}$$

where d_{opt} represents the optimal transmission range, d_{max} represents the estimated maximum transmission range for an acceptable error rate, and d_{trans} represents the translation distance ($d_{trans} = 150$ m for f_{trans} in Fig. 7). These parameters may be adjusted based on the network conditions in the area.

The *received power* p_i of a node N_i is the received power level of the RTS frame. Priority is given to nodes with stronger p_i. This parameter indicates the true channel quality from a sender to a receiver. Empirical studies and theoretic analysis can provide an optimal transmission area, but in reality, there can be obstacles or noise around nodes. The received power can also help in differentiating nodes at comparable distances. The fact that the reporting of the received signal power is made while the vehicles are moving does not affect the quality of the reported data, because the distance a vehicle travels while receiving an RTS is negligible.

2) Function definition: We adapt the multivariable function in [33] and customize it to a three-variable polynomial of the selected parameters. The waiting time t_i returned by this function is in the interval $[0, T_{\max}]$, where $T_{\max}$ is the maximum waiting time. We have

$$f(d_i, d_{SN_i}, p_i) = A d_i^{\alpha_1} f_i^{\alpha_2} p_i^{\alpha_3} + T_{\max}$$

where $A = (-T_{\max}/(d_{\max}^{\alpha_1} f_{\max}^{\alpha_2} p_{\max}^{\alpha_3}))$, and $\alpha_i (i = 1, 2, 3)$ is the weight of each parameter.

The greater the weight value is, the greater the impact that the parameter has in the election process. All next-hop candidates use the same values of parameters α_i. We currently use static values for these factors, but they could dynamically be determined and adjusted based on the network and traffic conditions in the area.

3) Function evaluation: Fig. 8 shows a comparison between the next-hop selection that uses the multicriterion function and the selection that uses only the forward-progress parameter. We consider a transmitter at location (0, 0) and a destination at location (800, 200). The waiting time for the nodes after they receive an RTS frame if they were located at various locations around the transmitter is shown in Fig. 8(a) and (b). In this comparison, we used the following coefficients in the multicriterion function: 1) $\alpha_1 = 0.2$, 2) $\alpha_2 = 1.2$, and 3) $\alpha_3 = 0.03$. The optimal wireless transmission range is set to be 250 m, and the translation function f_{trans} in Fig. 7 is deployed. Note that perfect reception within a specific range around the transmitter is not assumed. Rather, the received power is calculated using the shadowing propagation model [35]. In this model, the power level at a receiving node is not solely a function of the distance to the transmitting node, but randomness is added to account for fluctuations in signal propagation. The formula for computing the received power is

$$\left|\frac{P_r(d)}{P_r(d_0)}\right|_{\mathrm{dB}} = -10\beta \log\left(\frac{d}{d_0}\right) + X_{\mathrm{dB}} \tag{1}$$

where X_{dB} is a normal random variable with mean zero and standard deviation σ_{dB}. σ_{dB} is the shadowing deviation, and β represents the path-loss exponent.

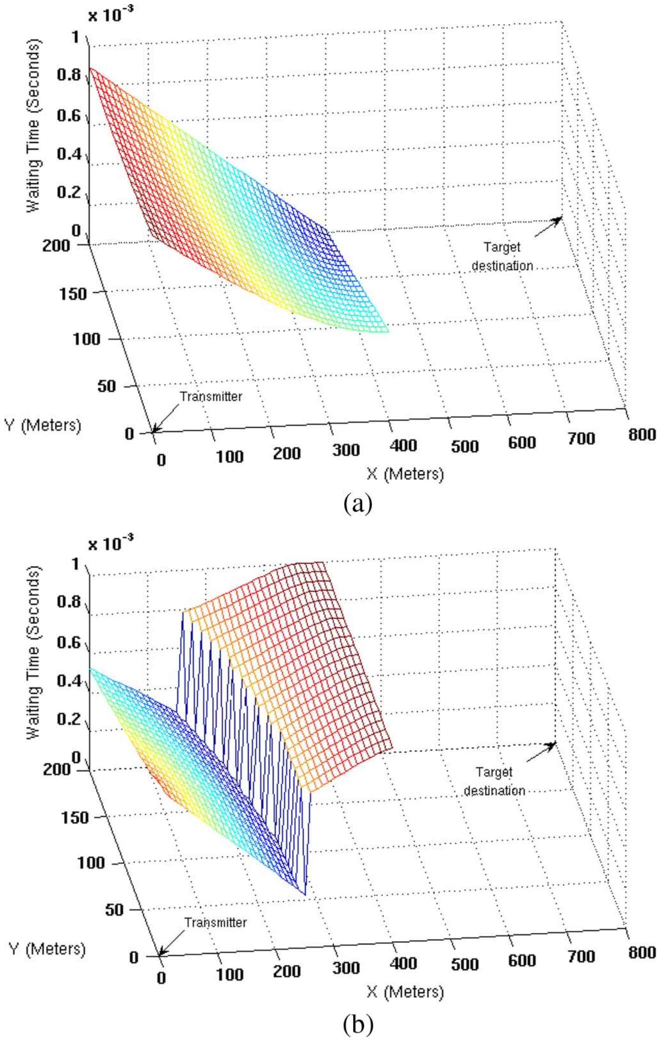

(a)

(b)

Fig. 8. Waiting times that were experienced by receivers located at various positions around a transmitter. (a) Waiting time that was determined using forward progress only. (b) Waiting time that was determined using the multicriterion function.

TABLE I
USING THE MULTICRITERION FUNCTION TO SELECT NEXT HOPS LEADS TO SIGNIFICANTLY LOWER PACKET LOSS AND OVERHEAD COMPARED WITH USING FORWARD PROGRESS ONLY

	Packet Loss Rate (%)	**Ratio of Frames per Received Packet**
Forward progress only	37.54%	36.50
Multi-criteria function	7.52%	2.62

The comparison in Fig. 8 shows that the proposed scheme favors nodes around the optimal transmission range and assigns shorter waiting times for the nodes within this range. The forward-progress-only approach favors nodes beyond the optimal transmission range (in case they receive the RTS), which could lead to many data packet losses. Table I validates this observation, because it presents a comparison between the two methods in terms of packet loss and the number of MAC-layer frames that were transmitted in the network per data packet that was successfully received at destinations (which is a measure of traffic overhead). These simulation results were obtained using RBVT-R in a network with 250 nodes. Fifteen source–destination pairs exchanged 10 000 packets at the rate of 2 packets/s. Using the multicriterion function leads to a packet loss that is five times lower than using forward progress only. In addition, the traffic overhead is more than one order of magnitude lower when using the proposed scheme. This result is due, in part, to the large number of retransmissions that were experienced by nodes located farther from the optimal transmission range.

IV. Performance Evaluation

This section presents the evaluation of the RBVT protocols using the network simulator NS-2.30 [36]. To evaluate the performance, we use two urban scenarios: 1) a scenario with obstacles to model buildings, in which we make use of periodic "hello" messages and the IEEE 802.11 with DCF standard, and 2) a scenario without obstacles to simulate high-contention networks, for which optimized forwarding is used. We compare RBVT-R and RBVT-P with four existing VANET/MANET routing protocols. In the following, we present the evaluation methodology, the metrics for comparing the protocols, and the analysis of the simulation results.

A. Evaluation Methodology

We compare the performance of the RBVT protocols with representatives from the main classes of routing protocols:

1) AODV [8], which is a MANET reactive routing protocol;
2) OLSR [28], which is a MANET proactive routing protocol;
3) GPSR [12], which is a MANET geographical routing protocol;
4) GSR [6], which is a VANET position-based routing protocol that takes into account the road layouts in the forwarding decisions.

We now briefly review how each of these protocols operate.

In AODV, a route is created on demand when a source node wants to communicate with a destination node. The route creation involves flooding a route request message and establishing, at each hop, a backward pointer (the last transmitter of the request) to the source. A reply is unicast along this path by using the backward pointers while establishing forward pointers to the destination. In OLSR, each node maintains sets of one- and two-hop neighbors and selects some neighbors as multipoint relays. OLSR proactively discovers and disseminates link-state information over the multipoint relays backbone. Using this topology information, each node computes the next hop to every other node in the network by using shortest path hop-count forwarding. GPSR is a position-based routing protocol that uses greedy geographical forwarding from the source node to the destination node. When a node cannot find a neighbor node that is closer to the destination position than itself, a recovery strategy based on planar graph traversal is applied. In GSR, every vehicle node is equipped with a GPS receiver and holds a digital map of the region. A source vehicle that wishes to communicate with a destination vehicle creates the shortest path based on the roads layout from its position to the destination position. This route is made of a sequence of road intersections. Data packets are forwarded using greedy geographical forwarding along this path. No consideration is given to the vehicular traffic.

B. Metrics

The performance of the routing protocols was evaluated by varying the data rate, the network density, and the number of concurrent user datagram protocol (UDP) flows. The metrics to assess the performance are given as follows.

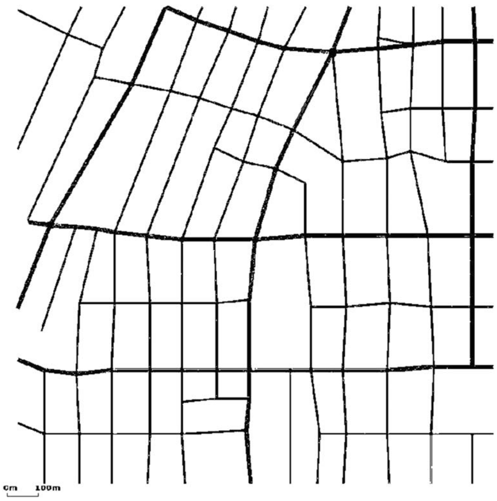

Fig. 9. Map of the region of Los Angeles, CA, used in the simulation scenario with obstacles.

- **Average delivery ratio.** This metric is defined as the number of data packets that were successfully delivered at destinations per number of data packets that were sent by sources (duplicate packets that were generated by loss of acknowledgments at the MAC layer are excluded). The average delivery ratio shows the ability of the routing protocol to successfully transfer data on an end-to-end basis.
- **Average delay.** This metric is defined as the average delay incurred in the transmission of all data packets that were successfully delivered. The average delay characterizes the latency that the routing approach generated.
- **Average path length.** This metric is defined as the average number of nodes that participated in the successful forwarding of packets from the source to the destination. Historically, the average path length was a measure of path quality. We use this metric to verify if there is a correlation between the path length, average delivery ratio, and average delay, respectively.
- **Overhead.** This metric is defined as the number of extra routing packets per number of unique data packets that were received at destinations. The overhead measures the additional traffic that the routing protocol generated for packets that were successfully delivered.

C. Simulation Results in the Scenario With Obstacles

1) Simulation Setup: The first simulation scenario is a 1500 m × 1500 m area that was extracted from the TIGER/Line database of the US Census Bureau [21]. Fig. 9 shows the map used. We used the open-source microscopic space-continuous time-discrete vehicular traffic generator package SUMO [18] to generate the movements of the vehicle nodes. SUMO uses a collision-free car-following model to determine the speed levels and the positions of the vehicles. We input into SUMO the map extracted from the Tiger/Line database and the specifications about the speeds limits and the number of lanes of each road

TABLE II
SIMULATION SETUP

Parameter	Value
Simulation area	1500m x 1500m
Number of vehicles	150-250-350
Number of CBR sources	1-20
Transmission range	400m
Simulation time	300s
Vehicle velocity	25 - 55 miles per hour
CBR rate	0.5 - 5 packet per second
MAC protocol	IEEE 802.11 DCF
Data packet size	512 bytes

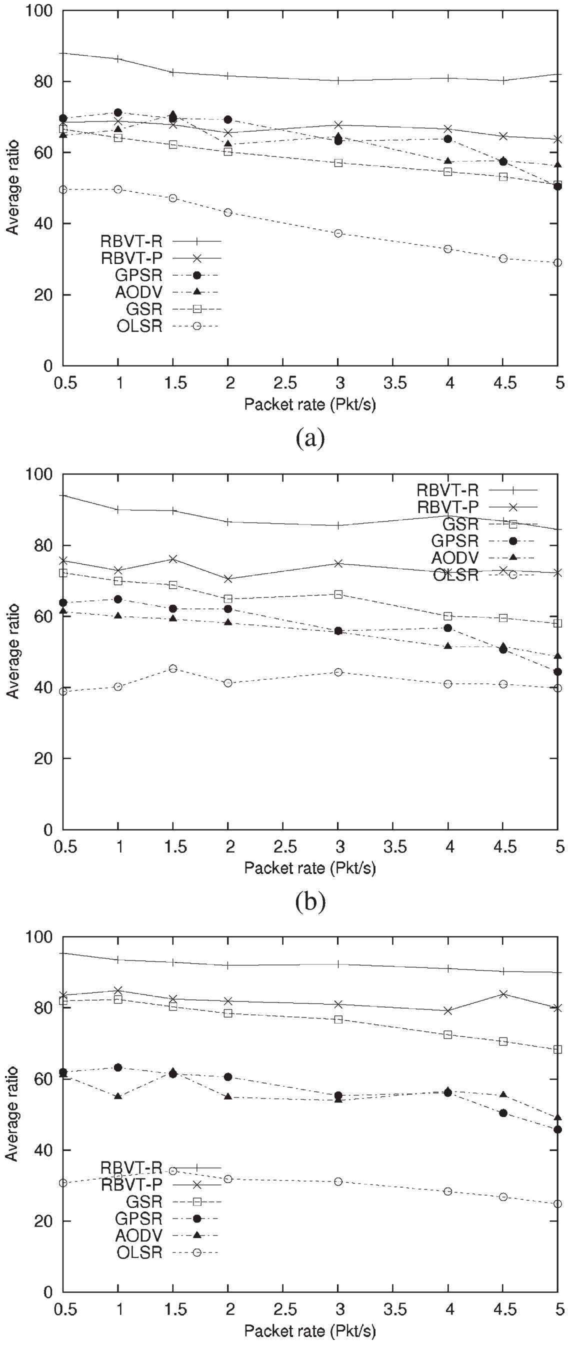

(a)

(b)

(c)

Fig. 10. Average delivery ratio for RBVT-R, RBVT-P, AODV, OLSR, GPSR, and GSR in networks with 15 flows and different node densities. (a) One hundred fifty nodes. (b) Two hundred fifty nodes. (c) Three hundred fifty nodes.

segment on the map. We also specified traffic-light-operated intersections and priority intersections (i.e., less than one-fifth of the intersections are regulated using traffic lights). We discard the first 2000 s of the SUMO output to obtain more accurate node movements. The output from SUMO is converted into input files for the movement of nodes in the NS-2 simulator.

For the wireless configuration, we used the IEEE 802.11 with DCF standard [22] at the MAC layer. At the physical layer, we used the shadowing propagation model to characterize physical propagation. We set a communication range of 400 m with an 80% probability of success for transmissions. These values were selected based on studies (e.g., [37]) that reported real-life measurements between moving vehicles in the range 450–550 m. In addition, although the DSRC standard specifies a range of up to 1000 m for safety applications, many nonsafety applications are expected to reach 400 m [23]. The values of path loss exponent $\beta = 3.25$ and deviation $\sigma = 4.0$ are used for the shadowing propagation [35].

We simulate buildings in a city environment using the following obstacle model. The contour of each street can either be a building wall (of various materials) or an empty area. Thus, for each street border, we set a signal attenuation value that was randomly selected between 0 and 16 dB. This attenuation is added to the signal attenuation that was determined by the shadowing propagation model in NS2. We found that the signal attenuation values that were obtained were comparable with values reported from field experiments at 5.3 GHz [38]. The simulation parameters are summarized in Table II.

We ran experiments in networks with different node densities: 1) the 350-node scenario represents relatively dense networks, 2) the 250-node scenario represents medium-density networks, and 3) the 150-node scenario represents sparse networks. The implementation of AODV was provided by NS-2.30 (with link-layer feedback being enabled), whereas the implementation of GSR is based on [6]. The GPSR implementation code is taken from [39], and the OLSR implementation code is taken from [40]. To allow the vehicle nodes to have more accurate neighbor information, we set the hello interval to 0.8 s and purge neighbors from the cache after 1.6 s of inactivity. The topology control interval in OLSR was set to 2 s.

2) Simulation Results:

Average delivery ratio: Fig. 10 shows that RBVT-R outperforms the other protocols, with as much as a 40% increase compared with AODV and as much as 30% increase compared with GSR. For most cases, we observe a decrease in the average delivery ratio as the data traffic increases. The descending slope is not acute, which means that the protocols can cope with the offered load. This result is partly due to the presence of obstacles on the map area, which limit the level of contention in the wireless network. RBVT-P performs better in medium and dense networks than in sparse networks. The reason is that, when the density is small [see Fig. 10(a)], network partitions prevent the CPs from covering large sections of the map, thus limiting the information gathered by the CPs.

Across network densities, we observe that the delivery ratio of protocols that integrate road layouts (i.e., RBVT protocols and GSR) increases as the network becomes denser. Both RBVT protocols perform better than GSR for all the densities, because they integrate real-time knowledge of the vehicular traffic on the roads. When the network is sparse, GSR does not perform as well as some node-centric protocols [see Fig. 10(a)]. However, as the node density increases, the shortest path along the roads map becomes more likely to have enough nodes; thus, there is an increase in the average delivery ratio.

Higher node densities do not necessarily mean improved performances for protocols that do not consider the road layouts. For example, in OLSR, the increase in the number of nodes translates into an increase of the link state updates. Two observations can be made on GPSR. First, given that city roads include irregularities such as dead-end streets, following the shortest Euclidean distance is not always equivalent to following the shortest path through the roads. Second, the GPSR protocol is stateless, and this condition generally provides many advantages for the routing of data packets. However, if a local maxima forms in the network, the stateless nature of the protocol means that packets will follow the same path to the position of the local maxima, and once there, the forwarding mode of each packet will be set to perimeter forwarding. This case is unlike protocols that implement feedback mechanisms, e.g., AODV, which can perform a local repair or send a route error notification to the data source node.

Average delay: Fig. 11 shows that RBVT-P has the smallest average delay among the protocols studied. RBVT-P performs better than RBVT-R due to the proactive-versus-reactive nature of the two protocols. In RBVT-P, the routes already exist during data transmission, whereas in RBVT-R, RD processes are started. Furthermore, the cost of gathering and disseminating routes in RBVT-P is shared among all the data flows, whereas in RBVT-R, each new flow adds its own routing cost. Thus, unlike in MANETs, proactive road-based protocols with real-time traffic awareness can be a viable approach in vehicular networks, particularly for delay sensitive applications such as video streaming.

We also observe that the average delay for RBVT-P consistently remains less than 1 s, whereas the average delay of RBVT-R decreases with the increase in density. The reason for this case is that RBVT-R routes remain active for longer periods of time (as the number of nodes increases). Thus, fewer packets need to be buffered, because the source repairs the route. The average delay of GSR, on the other hand, continually increases, because GSR forwards data on road segments that were solely selected based on the positions of the communication endpoints. A side effect to this step is that some road segments may become congested; however, because there is no communication quality feedback that is sent back to the source vehicle, the overall communication performance suffers. This result suggests that altering the paths used in GSR by using feedback from the network may improve the protocol performances.

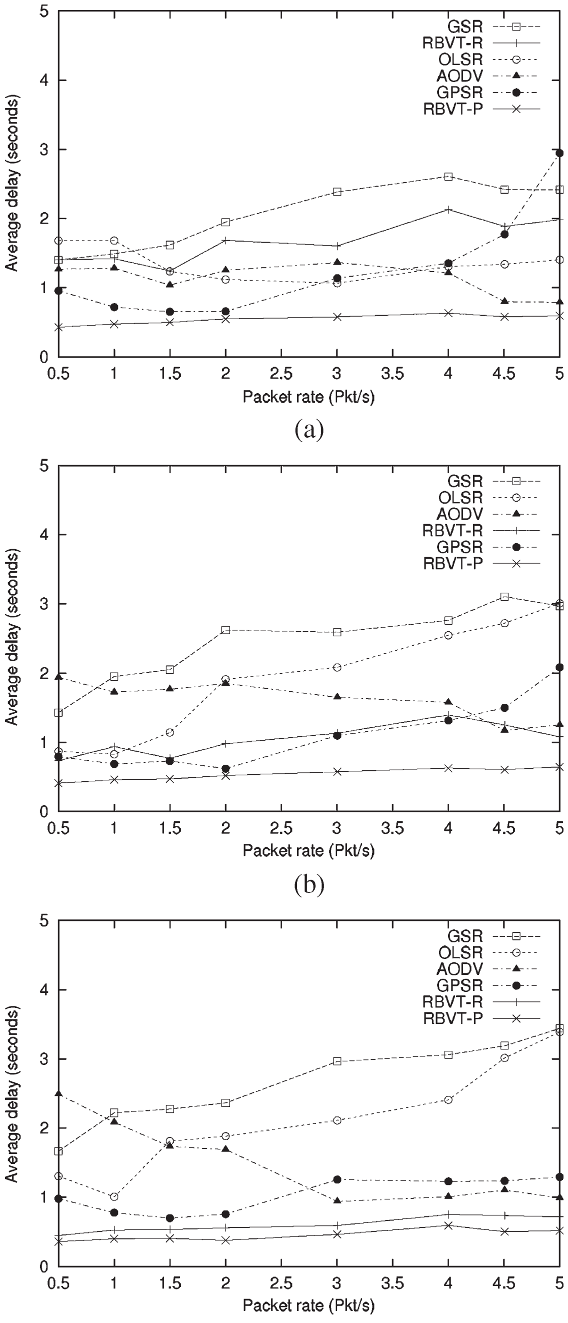

(a)

(b)

(c)

Fig. 11. Average delay for RBVT-R, RBVT-P, AODV, OLSR, GPSR, and GSR in networks with 15 flows and different node densities. (a) One hundred fifty nodes. (b) Two hundred fifty nodes. (c) Three hundred fifty nodes.

Average path length: Fig. 12(a) plots the average path length of packets that were received at the destination for the protocols. This plot is similar for different network densities, and we only present the results with 250 nodes. RBVT-R has longer average paths than the other protocols. There are two reasons for this result: 1) RBVT-R gives preference to link quality over forward progress when selecting the next neighbor node, and 2) unlike RBVT-P, which consistently selects the shortest connected path, a route that was established with RBVT-R is used until the source considers it broken, even if shorter routes form at a later time. This case suggests that RBVT-R can benefit from a method of assessing the quality of the routes used for communications, even when they are not broken. In addition, we note that longer path lengths do not necessarily translate, as could be expected, into worse performance. On the contrary, selecting better forwarding nodes

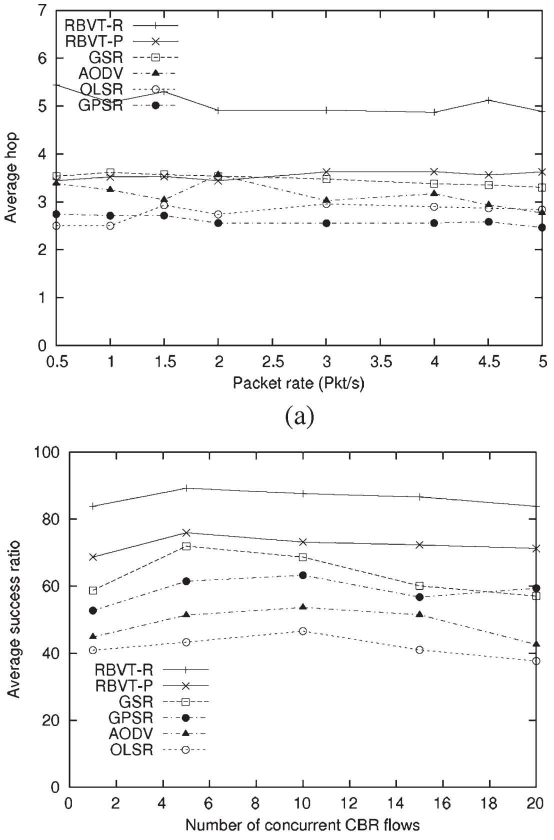

(a)

(b)

Fig. 12. (a) Average path length for variable data-sending rates and (b) average delivery ratio with a variable number of concurrent flows. The data rate in (b) is fixed at 4 packets/s, and the network size is 250 nodes.

leads to better performance (e.g., RBVT-R has the highest delivery ratio despite having longer paths).

Impact of the number of flows: The impact of the number of concurrent flows on the protocols' performance is shown in Fig. 12(b). The packet sending rate is 4 packets/s. RBVT protocols perform best in terms of delivery ratio. We observe that all the protocols scale well with the increase in the number of CBR flows in this scenario. The drop in performance is small, i.e., from 1 to 20 CBR pairs. All protocols that we have considered sustained sufficient multiple concurrent flows. We also compared running M flows with data rate N packet/s versus running N flows with data rate M packet/s. We observed that the performance is slightly better when we have more flows (and lower data rates per flow) because the traffic is more evenly distributed across the network.

D. Simulation Results in the Scenario Without Obstacles

1) Simulation Setup: Our second simulation scenario uses a 1500 m × 1500 m area that was extracted from the TIGER/Line database of the U.S. Census Bureau [21], which forms a grid layout with a total of 22 road segments. It is an area of Fellsmere, FL, with center point coordinates latitude 27.784728° North and longitude −80.604385° West. We set bidirectional traffic on each road, with two lanes in each direction. To evaluate the protocols under increased network congestion, we do not include obstacles in this scenario. This way, a small increase in the data-sending rate will provide a noticeable increase in the level of contention in the network.

We generate the vehicle movements using a microscopic mobility generator that we have developed based on the car-following and lane-changing models proposed by Gipps [19], [20]. The Gipps model belongs to the class of collision-avoidance vehicular mobility models. The main goal of these models is to allow a vehicle to move at the maximum safest speed that avoids collisions with the preceding vehicle. We target city scenarios; thus, our generator supports traffic lights at road intersections, as well as bidirectional and multilane traffic. The input to the generator is a map of the roads with specifications of the average speed and the average traffic flow on each road. When a vehicle enters a road segment, we determine its action at the end of the segment (i.e., left turn, right turn, u turn, or straight ahead) based on the average traffic flows of the roads crossing the end intersection. We discard the first 2000 s of the output to obtain more accurate movements of nodes.

We used the IEEE 802.11 with DCF standard for AODV, OLSR, GPSR, and GSR, and the forwarding optimizations for the RBVT protocols. We set the "hello" interval to 2 s, because it provided better results in this scenario. At the physical layer, we used the shadowing propagation model to characterize physical propagation. For these simulations, the wireless range is set to 250 m to prevent communication between vehicles on parallel streets (the minimum distance between streets is 400 m). In the simulations, we set the exponents for the waiting function in the next-hop self-election mechanism to $\alpha_1 = 0.07$, $\alpha_2 = 0.5$, and $\alpha_3 = 0.03$. We use the last-in–first-out (LIFO) queuing instead of the first-in–first-out (FIFO) queuing for RBVT in this scenario because it provided better latency when experiencing high contention [41].

2) Simulation Results:

Average delivery ratio: Fig. 13 shows that the RBVT protocols outperform the other protocols. We note that all the protocols are more sensible to the increase in the data rate. Both RBVT protocols perform better than the other protocols under added congestion because of the forwarding optimization. At 3 packet/s, for example, only RBVT-R and RBVT-P have a data delivery ratio above 50%. Comparing RBVT-P with OLSR, we observe that OLSR performance is more affected by contention in the network. RBVT-P maintains only the overall connectivity between the road intersections in the network, whereas OLSR proactively maintains the link state between the multipoint relays.

Average delay: Fig. 13(b) shows that, for most packet rates, RBVT-P has the best performance in terms of delay. The contention on the wireless channel can clearly be observed here, with the values of the average delay for GPSR and GSR increasing well above 5 s.

Impact of number of flows: The impact of the number of concurrent flows on the protocol performances in this scenario is shown in Fig. 14. In general, the fewer the number of flows, the better the protocol performance in terms of delivery ratio. Among the protocols, the RBVT protocols scale better than the other protocols. AODV shows the most accentuated drop in delivery ratio, with a 50% decrease from the 1-flow simulation to the 20-flow simulation. AODV protocol can keep the average

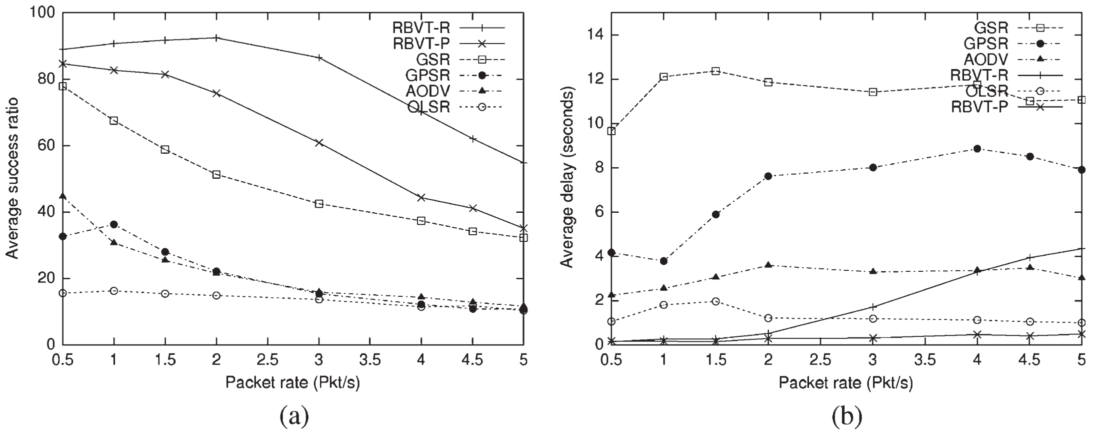

(a) (b)

Fig. 13. Average delivery ratio and average delay for RBVT-R, RBVT-P, AODV, OLSR, GPSR, and GSR in networks under high contention. (a) Average delivery ratio over 250 nodes. (b) Average delay over 250 nodes.

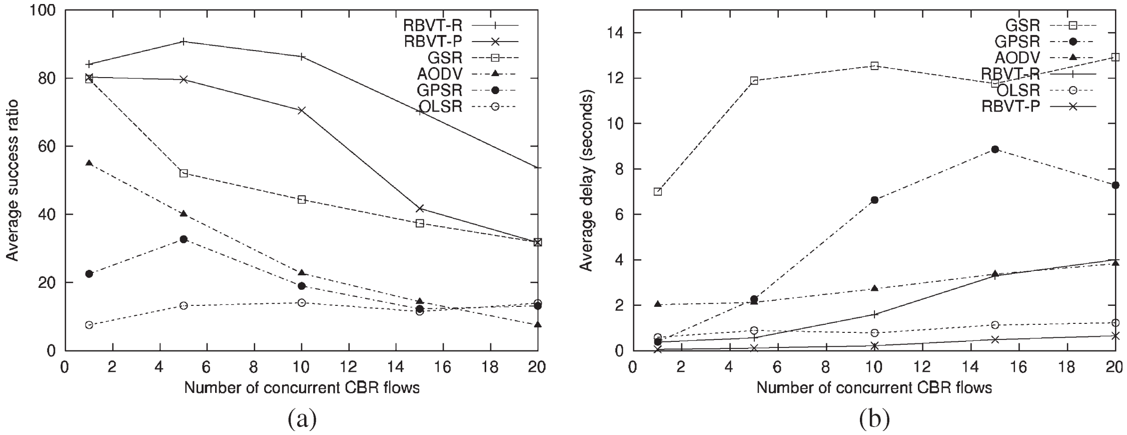

(a) (b)

Fig. 14. Average delivery ratio and average delay with varying numbers of concurrent flows. The data rate is fixed at 4 packets/s, and the network size is 250 nodes. (a) Average delivery ratio. (b) Average delay.

delay of the transmitted data in check by dropping packets for which it does not have a route. GSR does not scale very well with the variation in the number of flows either, particularly for the delay that practically doubles for 20 flows compared with one flow. RBVT-R has the minimum decrease in delivery ratio among the simulated protocols [see Fig. 14(a)]. However, RBVT-R's average delay is more sensitive to the added flows than RBVT-P's, which consistently maintains a small average delay.

Overhead: As expected, based on the results in Table I, the next-hop self election mostly eliminates the overhead of the RBVT protocols compared with other protocols such as AODV and GSR. Although RBVT-R floods RD requests and RBVT-P floods the routing update packets, these overheads are very small compared with the overhead introduced by frequent route errors in AODV and the "hello" packets overhead in GSR. Using the roads layout and the real-time vehicular traffic information leads to more stable paths and, hence, lower overhead for RBVT protocols.

E. Simulation Results of Forwarding Optimization

Figs. 15 and 16 assess the impact on performance of the proposed geographical forwarding mechanism, which takes advantage of the 802.11 RTS/CTS to choose the next hop using receiver self election, compared with a traditional approach that uses "hello" packets to create the list of neighbors at nodes. We consider both scenarios with and without obstacles and both RBVT protocols. For brevity, we show RBVT-R results using the map without obstacles and RBVT-P results using the map with obstacles.

In the scenario without obstacles, the "hello" packets were generated every 2 s. Fig. 15(a) shows that the forwarding optimization leads to a delivery ratio as much as three times higher in congested environments. Similarly, Fig. 15(b) shows that the delay is three times lower, on the average, with the improvements. There are two reasons for these high improvements. First, the absence of periodic hello messages means less overhead in the network. This overhead reduction leads to much higher link utilization for data transfers. It also leads to improved delays, because fewer retransmissions and exponential backoffs are necessary. Second, the multicriterion waiting function that was used in the election of the next hop favors link quality over greediness, as explained in Section III-C.

In the scenario with obstacles [see Fig. 16(a)], the forwarding optimizations lead to an increase in the packet delivery ratio of up 14%. The difference between the self-election and the selection results in this scenario is smaller compared with the

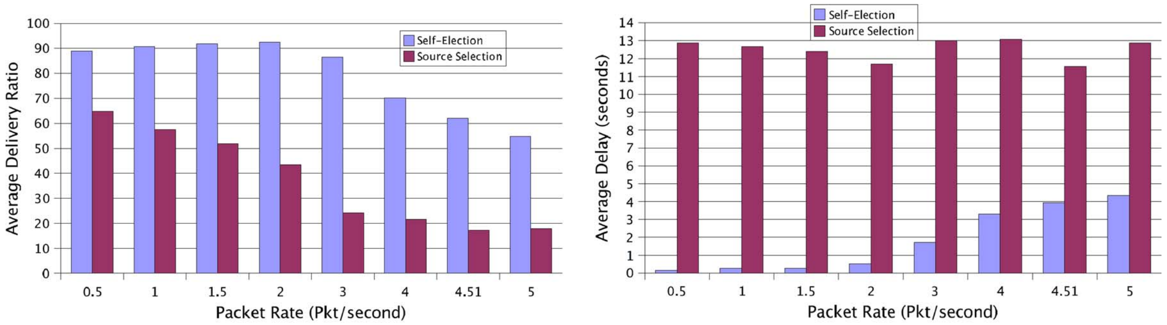

(a)

(b)

Fig. 15. Average delivery ratio and average delay comparison between two types of geographical forwarding, source selection using "hello" packets, and receiver self-election using our RTS/CTS-based mechanism under the scenario without obstacles. The routing protocol is RBVT-R, and the network size is 250 nodes. (a) Average delivery ratio. (b) Average delay.

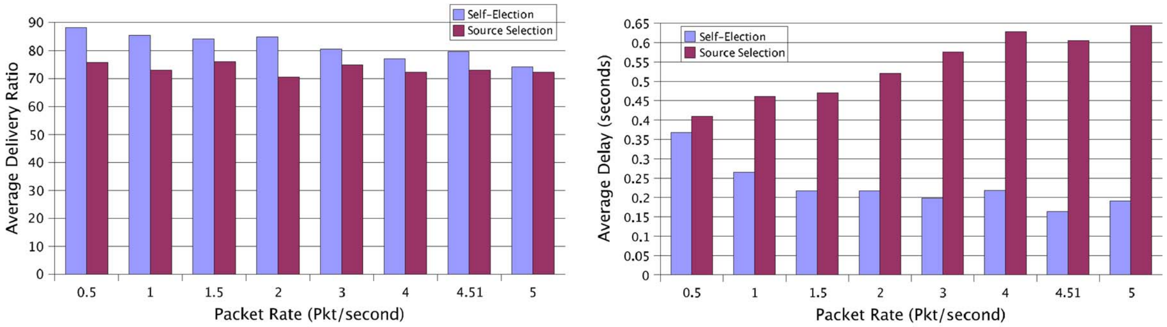

(a)

(b)

Fig. 16. Average delivery ratio and average delay comparison between two types of geographical forwarding, source selection using "hello" packets, and receiver self-election using our RTS/CTS-based mechanism under the scenario with obstacles. The routing protocol is RBVT-P, and the network size is 250 nodes. (a) Average delivery ratio. (b) Average delay.

scenario without obstacles [see Fig. 15(a)]. This result is due to the reduced level in contention because of the obstacles. The average delay is also reduced.

F. Simulation Results of RBVT-P CPs

In our final simulations, we analyze the parameters that influence the accuracy of the connectivity view of the nodes in RBVT-P: 1) the number of CPs generated per period; 2) the geographical dispersion of the CP initiators; and 3) the interval between generation of CPs. For this study, we employ the scenario with obstacle and the IEEE 802.11 DCF standard at the MAC layer. Unless otherwise specified, we used 250 nodes in the simulations, and the CP interval was set at 10 s. A node generates a CP after the following instances: 1) It verifies that it has not received any CP update for a period that is at least equal to the CP interval, and 2) it executes a Boolean function, for which the return value is determined based on the number of desired CPs. We measure the percentage of false negatives between pairs of vehicle nodes, i.e., the difference between the nodes' local connectivity view and the simulator global connectivity view for every pair of nodes in the network.

1) Number of CPs: To understand the impact of the number of generated CPs on the accuracy of the connectivity map, we ran simulations with different numbers of CPs. In this test, the nodes that generate the CPs were randomly selected, regardless of their relative positions on the map.

TABLE III
FALSE NEGATIVES WITH THE NUMBER OF CPS

	1 CP	2 CPs	5 CPs	10 CPs
False-negative	28.51%	20.36%	14.73%	11.44%

Table III shows that, as the number of CPs generated in the network increases, the number of false-negative information between vehicle pairs substantially decreases. Considering that there is a tradeoff between a complete real-time view and the amount of CPs that would be required to generate it, we select three CPs as a good tradeoff between accuracy and overhead for this map size and features.

2) Interval Between CP Generation: Next, we assess the impact of the CP interval (i.e., the time between the generation of new CPs in the network). Five vehicles are randomly selected to create CPs, and the number of vehicle nodes is 350.

The percentage of false negatives was 47.60% when the interval between CP was 5 s and 9.13% when the interval between CP was 10 s. One would have expected that a lower CP generation interval would lead to better results. However, this is not the case, because it also leads to higher overhead, which, in turn, leads to more packet drops. The significant difference between 5and 10-s intervals suggests that an inadequate selection of this parameter can adversely affect the RBVT-P protocol's performance.

3) Distribution of CP Generator: Our final test assesses the influence of the geographical distribution of the CP initiators

TABLE IV
FALSE NEGATIVES AND THE POSITIONS OF CP INITIATORS

	Near	Spread
False-negative	25.51%	15.04%

on the accuracy of the connectivity information. For this test, we position three static vehicles at specific positions in the map area. In the "Near" case, the vehicles are positioned close to one another, and in the "Spread" case, the vehicles are spread on the map area.

As expected, Table IV shows that, when the CP initiators are spread on the map, the quality of the connectivity information improves. The fact that the vehicles used in the "Spread" simulation were not moving does not seem to have a noticeable impact. Its results are comparable with those in Table III, where moving vehicles were used.

V. Related Work

Routing has been a major research topic in MANETs. AODV [8], DSDV [42], DSR [9], and OLSR [28] are node-centric MANET protocols in which topological end-to-end paths are created. To improve on their performance in VANETs, solutions have been proposed, which exploit the knowledge of relative velocities between nodes and the constrained movements of vehicles [43]–[45]. This information is used to select nodes with high relative velocity to the destination, predict the lifetime of routes, or reduce the number of route breaks by selecting, during the route creation, nodes that move in the same direction and with a small relative speed. RBVT routing differs from these protocols in that the routes are road based, and their main components are the road intersections that were traversed on the path from the source to the destination.

Geographical routing protocols, e.g., GPSR [12], GFG [10], and GOAFR [11], use node positions to route data between endpoints. When a local maxima is reached (i.e., a position where progress cannot be made based on node positions), recovery strategies are proposed to route the packets around the void. Solutions in [46] and [47] propose to improve recovery strategies in VANETs by either proactively detecting potential dead-end positions or using channel overhearing capabilities of wireless networks to decrease the number of hops on the recovery paths.

The concept of anchor-based routing in sensor networks [48], [49] has been adopted to VANET environments. GSR [6] and SAR [14] integrate the road topologies in routing using those concepts. In these protocols, a source computes the shortest road-based path from its current position to the destination. Similar to RBVT, they include the list of intersections that define the path from the source to the destination in the header of each data packet that was sent by the source. However, they do not consider the real-time vehicular traffic, and consequently, they could include empty roads. To alleviate this issue, A-STAR [50] modifies GSR by giving preference to streets served by transit buses each time a new intersection will be added to the source route. CAR [7] finds connected paths between source–destination pairs, considering vehicular traffic, and uses "guards" to adapt to movements of nodes. Gytar [15] dynamically adds intersections, choosing the next road segment with the best balance of road density and road length.

MDDV [17] and VADD [16] use opportunistic forwarding to transport data from the source to the destination in VANETs. VADD uses historic data traffic flow to determine the best route to the destination. MDDV considers the road traffic conditions and the number of lanes on each road segment to select the best road-based trajectory to forward data. In both protocols, when no vehicle node can be found along the forwarding trajectory, a carry-and-forward approach is used, and the data packets are stored until a more suitable relay is found. These protocols are well suited for delay-tolerant applications (i.e., applications for which the users can tolerate a certain level of delay, as long as the data eventually arrives). A delay-tolerant epidemic routing approach for VANETs is presented in [51]. Under very sparse vehicular traffic and at the early stages of the deployment of wireless technology in vehicles (when many vehicles will not have wireless interfaces), such opportunistic forwarding solutions will be useful to car-to-car ad hoc communications. The RBVT protocols, on the other hand, provide support for applications that are not necessarily delay tolerant. RBVT protocols require that an end-to-end path exists for data to reach the destination.

Receiver-based next-hop selection is proposed at the routing layer (e.g., [29]) and at the MAC layer (e.g., [30]–[34]). In [29], all neighbors receive the entire packet, but only one neighbor will rebroadcast it. This neighbor is the one that wins a time-based contention phase in which the node closest to the destination is favored. Minimizing the remaining distance to the destination is also the objective in [30], [31], and [34], which operate at the MAC layer. These methods consider the unit-disk assumption, which does not hold in real-life VANETs. RBVT next-hop self election can work in realistic conditions, where obstacles and noise frequently affect wireless communication, because it incorporates multiple criteria in the selection of the best next hop (i.e., forwarding progress, optimal transmission area, and received power).

Multicriterion receiver-based next-hop selection has been described in a general form in [33]. The authors demonstrated that using carefully selected criteria can improve the election of the optimal next hop. We apply these results in the context of vehicular networks and define a set of criteria to optimize the election of the next hop.

We note that real-life measurements with commercial GPS receivers [52] showed errors in the reporting of GPS positions in urban environments. RBVT protocols follow paths made of road segments; thus, they are more resilient to vehicle node position errors of a few meters. The integration of the inertial navigation system into GPS receivers is expected to improve the detection and handling of GPS position errors.

VI. Conclusion

This paper has presented RBVT, which is a class of VANET routing protocols for city-based environments that takes advantage of the layout of the roads to improve the performance of routing in VANETs. RBVT protocols use real-time vehicular traffic information to create road-based paths between endpoints. Geographical forwarding was used to find forwarding nodes along the road segments that form these paths. To improve the end-to-end performance under high contention, we have also proposed a distributed next-hop self-election mechanism for geographical forwarding. Simulation results have shown that our two protocols, namely RBVT-R and RBVT-P, outperform existing approaches in terms of the average delivery ratio and average delay. The RBVT protocols forward data along the streets (not across the streets) and take the real traffic on the roads into account; thus, they perform well in realistic vehicular environments in which buildings and other road characteristics, e.g., dead-end streets, are present. These results show that distributed applications that generate a moderate amount of traffic can successfully be implemented in VANETs. Furthermore, these applications can use RBVT-R when throughput is their main requirement and RBVT-P if they are delay sensitive.

References

[1] S. Dashtinezhad, T. Nadeem, B. Dorohonceanu, C. Borcea, P. Kang, and L. Iftode, "Trafficview: A driver assistant device for traffic monitoring based on car-to-car communication," in *Proc. 59th IEEE Semiannual Veh. Technol. Conf.*, Milan, Italy, May 2004, pp. 2946–2950.

[2] P. Zhou, T. Nadeem, P. Kang, C. Borcea, and L. Iftode, "EZCab: A cab booking application using short-range wireless communication," in *Proc. 3rd IEEE Int. Conf. PerCom*, Kauai Island, HI, Mar. 2005, pp. 27–38.

[3] O. Riva, T. Nadeem, C. Borcea, and L. Iftode, "Context-aware migratory services in ad hoc networks," *IEEE Trans. Mobile Comput.*, vol. 6, no. 12, pp. 1313–1328, Dec. 2007.

[4] A. Nandan, S. Das, G. Pau, and M. Gerla, "Cooperative downloading in vehicular ad hoc wireless networks," in *Proc. 2nd Annu. IEEE Conf. WONS*, St. Moritz, Switzerland, Jan. 2005, pp. 32–41.

[5] CarTel, Mass. Inst. Technol., Cambridge, MA. [Online]. Available: http://cartel.csail.mit.edu

[6] C. Lochert, H. Hartenstein, J. Tian, H. Füßler, D. Hermann, and M. Mauve, "A routing strategy for vehicular ad hoc networks in city environments," in *Proc. IEEE Intell. Vehicles Symp.*, Columbus, OH, Jun. 2003, pp. 156–161.

[7] V. Naumov and T. Gross, "Connectivity-aware routing (CAR) in vehicular ad hoc networks," in *Proc. IEEE Int. Conf. Comput. Commun.*, Anchorage, AK, May 2007, pp. 1919–1927.

[8] C. E. Perkins and E. M. Royer, "Ad hoc on-demand distance vector routing," in *Proc. 2nd IEEE Workshop Mobile Comput. Syst. Appl.*, New Orleans, LA, Feb. 1999, pp. 90–100.

[9] D. B. Johnson and D. A. Maltz, "Dynamic source routing in ad hoc wireless networks," *Mobile Comput.*, vol. 353, no. 5, pp. 153–161, 1996.

[10] P. Bose, P. Morin, I. Stojmenovic, and J. Urrutia, "Routing with guaranteed delivery in ad hoc wireless networks," *ACM Wirel. Netw.*, vol. 7, no. 6, pp. 609–616, Nov. 2001.

[11] F. Kuhn, R. Wattenhofer, Y. Zhang, and A. Zollinger, "Geometric ad hoc routing: Of theory and practice," in *Proc. 22nd Annu. Symp. Principles Distrib. Comput.*, Boston, MA, Jul. 2003, pp. 63–72.

[12] B. Karp and H. T. Kung, "GPSR: Greedy perimeter stateless routing for wireless networks," in *Proc. 6th Annu. Int. MobiCom*, Boston, MA, Aug. 2000, pp. 243–254.

[13] T. Li, S. K. Hazra, and W. Seah, "A position-based routing protocol for metropolitan bus networks," in *Proc. 61st IEEE VTC—Spring*, Stockholm, Sweden, Jun. 2005, pp. 2315–2319.

[14] J. Tian, L. Han, K. Rothermel, and C. Cseh, "Spatially aware packet routing for mobile ad hoc intervehicle radio networks," in *Proc. IEEE Intell. Transp. Syst.*, Shanghai, China, Oct. 2003, pp. 1546–1551.

[15] M. Jerbi, R. Meraihi, S.-M. Senouci, and Y. Ghamri-Doudane, "Gytar: Improved greedy traffic aware routing protocol for vehicular ad hoc networks in city environments," in *Proc. 3rd ACM Int. Workshop VANET*, Los Angeles, CA, Sep. 2006, pp. 88–89.

[16] J. Zhao and G. Cao, "VADD: Vehicle-assisted data delivery in vehicular ad hoc networks," *IEEE Trans. Veh. Technol.*, vol. 57, no. 3, pp. 1910–1922, May 2008.

[17] H. Wu, R. Fujimoto, R. Guensler, and M. Hunter, "MDDV: A mobility-centric data dissemination algorithm for vehicular networks," in *Proc. 1st ACM Int. Workshop VANET*, Philadelphia, PA, Oct. 2004, pp. 47–56.

[18] Centre for Applied Informatics (ZAIK) and the Institute of Transport Research German Aerospace Centre, *Sumo—Simulation of Urban Mobility* (last accessed Jul. 2008). [Online]. Available: http://sumo.sourceforge.net/

[19] P. G. Gipps, "A behavioral car-following model for computer simulation," *Trans. Res. Board*, vol. 15, no. 2, pp. 105–111, Apr. 1981.

[20] P. Gipps, "A model for the structure of lane-changing decisions," *Trans. Res. Board*, vol. 20B, no. 5, pp. 403–414, Oct. 1986.

[21] U.S.Census Bureau—TIGER/Line 2006 Second ed. (last accessed Jul. 2008). [Online]. Available: http://www.census.gov/geo/www/tiger/

[22] Institute of Electrical and Electronic Engineers (IEEE), *Wireless LAN Medium Access Control (MAC) and Physical Layer Specifications*. [Online]. Available: http://standards.ieee.org/getieee802/802.11.html

[23] "Task 3 Final Report," *Identify Intelligent Vehicle Safety Applications Enabled by DSRC, DOT HS 809 859*, Mar. 2005 (last accessed Jul. 2008). [Online]. Available: http://www-nrd.nhtsa.dot.gov/pdf/nrd-12/1665CAMP3web/index.html

[24] S.-Y. Ni, Y.-C. Tseng, Y.-S. Chen, and J.-P. Sheu, "The broadcast storm problem in a mobile ad hoc network," in *Proc. 5th Annu. ACM/IEEE Int. Conf. Mobile Comput. Netw.*, Seattle, WA, Aug. 1999, pp. 151–162.

[25] L. Briesemeister and G. Hommel, "Role-based multicast in highly mobile but sparsely connected ad hoc networks," in *Proc. 1st Annu. Workshop MOBIHOC*, Boston, MA, Aug. 2000, pp. 45–50.

[26] Q. Sun, S. Y. Tan, and K. C. Teh, "Analytical formulae for path loss prediction in urban street grid microcellular environments," *IEEE Trans. Veh. Technol.*, vol. 54, no. 4, pp. 1251–1258, Jul. 2005.

[27] J. Li, J. Jannotti, D. S. J. De Couto, D. R. Karger, and R. Morris, "A scalable location service for geographic ad hoc routing," in *Proc. 6th ACM Int. Conf. MobiCom*, Boston, MA, Aug. 2000, pp. 120–130.

[28] T. Clausen and P. Jacquet, *Optimized Link State Routing Protocol (OLSR)*, 2003. [Online]. Available: http://hipercom.inria.fr/olsr/rfc3626.txt

[29] H. Füßler, J. Widmer, M. Käsemann, M. Mauve, and H. Hartenstein, "Contention-based forwarding for mobile ad hoc networks," *Ad Hoc Netw.*, vol. 1, no. 4, pp. 351–369, Nov. 2003.

[30] K. Egoh and S. De, "Priority-based receiver-side relay election in wireless ad hoc sensors networks," in *Proc. Int. Conf. Wireless Commun. Mobile Comput.*, Vancouver, BC, Canada, Jul. 2006, pp. 1177–1182.

[31] M. Chawla, N. Goel, K. Kalaichelvan, A. Nayak, and I. Stojmenovic, "Beaconless position-based routing with guaranteed delivery for wireless ad hoc and sensor networks," *Acta Autom. Sin.*, vol. 32, no. 6, pp. 847–855, Nov. 2006.

[32] G. Zhou, T. He, S. Krishnamurthy, and J. A. Stankovic, "Impact of radio irregularity on wireless sensor networks," in *Proc. 2nd Int. Conf. MOBISYS*, Boston, MA, Jun. 2004, pp. 125–138.

[33] K. Egoh and S. De, "A multicriteria receiverside relay election approach in wireless ad hoc networks," in *Proc. MILCOM*, Washington, DC, Oct. 2006, pp. 1–7.

[34] M. Zorzi and R. R. Rao, "Geographic random forwarding (GERAF) for ad hoc and sensor networks: Multihop performance," *IEEE Trans. Mobile Comput.*, vol. 2, no. 4, pp. 337–348, Oct.–Dec. 2003.

[35] T. S. Rappaport, *Wireless Communications Principles and Practice*. Englewood Cliffs, NJ: Prentice–Hall, 1996.

[36] *The Network Simulator: NS-2*. [Online]. Available: http://www.isi.edu/nsnam/ns

[37] N. Eude, B. Ducourthial, and M. Shawky, "Enhancing ns-2 simulator for high mobility ad hoc networks in car-to-car communication," in *Proc. 7th IFIP Int. Conf. Mobile Wireless Commun. Netw.*, Marrakech, Morocco, Sep. 2005.

[38] X. Zhao, T. Rautiainen, K. Kalliola, and P. Vainikainen, "Path-loss models for urban microcells at 5.3 GHz," *IEEE Antennas Wireless Propag. Lett.*, vol. 5, no. 1, pp. 152–154, Dec. 2006.

[39] B. Karp, *Greedy Perimeter Stateless Routing (GPSR)* (last accessed Jul. 2008). [Online]. Available: http://www.icir.org/bkarp/gpsr/gpsr.html

[40] HIPERCOM, INRIA, *Optimized Link State Routing Protocol (OLSR)* (last accessed Jul. 2008). [Online]. Available: http://hipercom.inria.fr/olsr/

[41] J. Nzouonta, T. Ott, and C. Borcea, *Impact of Queue Discipline on Streaming Latency in Ad Hoc Networks*, submitted for publication.

[42] C. E. Perkins and P. Bhagwat, "Highly dynamic destination-sequenced distance-vector routing (DSDV) for mobile computers," in *Proc. ACM SIGCOMM Conf. Commun. Architectures, Protocols Appl.*, London, U.K., Sep. 1994, pp. 234–244.

[43] K.-T. Feng, C.-H. Hsu, and T.-E. Lu, "Velocity-assisted predictive mobility and location-aware routing protocols for mobile ad hoc networks," *IEEE Trans. Veh. Technol.*, vol. 57, no. 1, pp. 448–464, Jan. 2008.

[44] V. Namboodiri and L. Gao, "Prediction-based routing for vehicular ad hoc networks," *IEEE Trans. Veh. Technol.*, vol. 56, no. 4, pp. 2332–2345, Jul. 2007.

[45] T. Taleb, E. Sakhaee, A. Jamalipour, K. Hashimoto, N. Kato, and Y. Nemoto, "A stable routing protocol to support its services in VANETs," *IEEE Trans. Veh. Technol.*, vol. 56, no. 6, pp. 3337–3347, Nov. 2007.

[46] C.-H. Chou, K.-F. Ssu, and H. C. Jiau, "Geographic forwarding with dead-end reduction in mobile ad hoc networks," *IEEE Trans. Veh. Technol.*, vol. 57, no. 4, pp. 2375–2386, Jul. 2008.

[47] X. Ma, M.-T. Sun, G. Zhao, and X. Liu, "An efficient path pruning algorithm for geographical routing in wireless networks," *IEEE Trans. Veh. Technol.*, vol. 57, no. 4, pp. 2474–2488, Jul. 2008.

[48] L. Blazevic, L. Buttyan, S. Capkun, S. Giordano, J.-P. Hubaux, and J.-Y. L. Boudec, "Self-organization in mobile ad hoc networks: The approach of terminodes," *IEEE Commun. Mag.*, vol. 39, no. 6, pp. 166–174, Jun. 2001.

[49] L. Blazevic, S. Giordano, and J.-Y.-Y. L. Boudec, "Self-organized terminode routing," *J. Cluster Comput.*, vol. 5, no. 2, pp. 205–218, Apr. 2002.

[50] B.-C. Seet, G. Liu, B.-S. Lee, C.-H. Foh, K.-J. Wong, and K.-K. Lee, "A-star: A mobile ad hoc routing strategy for metropolis vehicular communications," in *Proc. NETWORKING*, Apr. 2004, vol. 3042, pp. 989–999.

[51] H.-Y. Huang, P.-E. Luo, M. Li, D. Li, X. Li, W. Shu, and M.-Y. Wu, "Performance evaluation of SUVnet with real-time traffic data," *IEEE Trans. Veh. Technol.*, vol. 56, no. 6, pp. 3381–3396, Nov. 2007.

[52] S. Savasta, M. Pini, and G. Marfia, "Performance assessment of a commercial GPS receiver for networking applications," in *Proc. IEEE Int. Consumer Commun. Netw. Conf.*, Las Vegas, NV, Jan. 2008, pp. 613–617.

Josiane Nzouonta received the M.S. degree in computer science from the Florida Institute of Technology, Melbourne, in 2003. She is currently pursuing the Ph.D. degree with the Department of Computer Science, New Jersey Institute of Technology, Newark.

Her research interests include wireless ad hoc networks, vehicular networks, and security in distributed systems.

Neeraj Rajgure received the M.S. degree in computer science from the New Jersey Institute of Technology (NJIT), Newark, in 2008.

His research interests include wireless sensor networks and vehicular networks.

Guiling (Grace) Wang (M'06) received the B.S. degree from Nankai University, Tianjin, China, and the Ph.D. degree in computer science and engineering, with a minor in statistics, from the Pennsylvania State University, University Park, in 2006.

She is currently an Assistant Professor with the Department of Computer Science, New Jersey Institute of Technology, Newark. Her research interests include distributed systems, wireless networks, and mobile computing, with emphasis on wireless sensor networks.

Cristian Borcea (M'02) received the Ph.D. degree in computer science from Rutgers University, Piscataway, NJ, in 2004.

He is currently an Assistant Professor with the Department of Computer Science, New Jersey Institute of Technology, Newark. His research interests include mobile computing, middleware, ad hoc networks, and distributed systems.

Dr. Borcea is a member of the Association for Computing Machinery and the Advanced Computing Systems Professional and Technical Association (Usenix).